Stationary patterns in a discrete bistable reaction–diffusion system: mode analysis*

Zou Wei(邹 为)[a)b)] and Zhan Meng(占 萌)[a)†]

[a)] *Wuhan Institute of Physics and Mathematics, the Chinese Academy of Sciences, Wuhan* 430071, *China*

[b)] *Graduate School of the Chinese Academy of Sciences, Beijing* 100049, *China*

(Received 18 January 2010; revised manuscript received 9 April 2010)

This paper theoretically analyses and studies stationary patterns in diffusively coupled bistable elements. Since these stationary patterns consist of two types of stationary mode structure: kink and pulse, a mode analysis method is proposed to approximate the solutions of these localized basic modes and to analyse their stabilities. Using this method, it reconstructs the whole stationary patterns. The cellular mode structures (kink and pulse) in bistable media fundamentally differ from stationary patterns in monostable media showing spatial periodicity induced by a diffusive Turing bifurcation.

Keywords: discrete reaction–diffusion system, stationary patterns, bistable, mode analysis

PACC: 0547, 4610

1. Introduction

Pattern formation[1−3] has become one of the most important fields in nonlinear science with the aim to understand how and why patterns appear, evolve, and interact in nature. So far, a variety of patterns have been observed and studied in disparate systems,[4−9] such as spiral waves in chemical reactions, epidemic waves in ecological communities, combustion waves in forest fire, excitation waves in cardiac tissue, propagation waves in cerebral cotex, etc. Obviously the dynamics of patterns is of great significance for system's function. As an example, in developmental biology, the pattern formation in space and time determines cell fates. Roughly speaking, all patterns can be classified into stationary pattern and wave pattern, with the former representing motionless and the latter evolving pattern with time. In this work, we will study stationary patterns in a discrete bistable reaction–diffusion system and reveal the rule for organization.

One of the well-known stationary patterns is the Turing pattern in monostable media,[10] which spontaneously appears from a homogeneous steady state due to a diffusion-induced instability. Turing pattern has been well observed in chemical experiments[11−14] and is expected to be a basis for morphogenesis in biological systems.

As opposite to this, in the studies of pattern formation in bistable (and multistable) media, much effort has been devoted to wave patterns — propagation traveling waves, as the waves of one stable phase can propagate into another stable phase.[5−7] Seemingly there is no room for stationary patterns. Nevertheless, extensive studies have well demonstrated that the dynamics in discrete bistable systems shows significant differences with that in continuous bistable systems, one of which is the occurrence of propagation failure,[15−22] i.e., propagation may fail in discrete bistable systems if the coupling is too small, whereas continuous systems allow for propagation at all coupling strengths. Correspondingly, stationary patterns still exist within a broad parameter region in discrete bistable systems.

So far, the stationary patterns in discrete bistable systems in the propagation-failure region have been extensively studied and reported in the literature.[23−26] For example, the existence of multiple stationary states under the weak coupling condition was studied in Ref. [23]. The multiplicity of rich pattern structures stems from the randomicity in initial conditions. In a chain of coupled bistable oscillators, the spatiotemporal behaviour with spatial chaos

*Project partially supported by the Outstanding Oversea Scholar Foundation of the Chinese Academy of Sciences (Bairenjihua) and the Scientific Research Foundation for the Returned Overseas Chinese Scholars, State Education Ministry.

†Corresponding author. E-mail: zhanmeng@wipm.ac.cn

© 2010 Chinese Physical Society and IOP Publishing Ltd

was analysed by a Henon-type map and related to the well-known Smale's horseshoe.[24] Recently, a detailed description of stationary patterns in one-, two-, and three-dimensional bistable reaction–diffusion media by Chua's circuit model was presented,[25] and reconstruction of some stable stationary approximate solutions was reported.[26] It is noticeable that most existing works concentrated on stationary solutions in discrete bistable systems in the limit of weak coupling and pursued approximate solutions. To the best knowledge of the authors, however, a systematical and quantitative study of stationary patterns in discrete bistable systems for any coupling strength (especially, strong one) is still missing. So far, an overall view of the structure, formation, and stability (and/or instability) of these patterns remains unclear. It is notable that this is an old but basic problem and the results could shed improved light on our understanding of pattern formation in coupled nonlinear systems.

2. Model and system properties

We consider the classical dimensionless discrete version of the Nagumo equation:[27]

$$\frac{\mathrm{d}x_i}{\mathrm{d}t} = f(x_i) + \varepsilon(x_{i+1} + x_{i-1} - 2x_i), \quad i = 1, \ldots, N, \tag{1}$$

where x_i is real variable representing the state of the i-th element at time t, N denotes the system size, ε is the diffusive coupling strength ($\varepsilon \geq 0$), and $f(x)$ is chosen as a nonlinear bistable function: $f(x) = -(x+1)(x-\alpha)(x-1)$ with $-1 < \alpha < 1$. Without losing generality, sufficiently large systems ($N \gg 1$) with periodic boundary conditions will be investigated. In the absence of coupling, a single element is bistable, with two stable steady states at $x = -1$ and $x = +1$, and one unstable steady state at $x = \alpha$. If $\alpha = 0$, it is a symmetric bistable system. The two steady states $x = -1$ and $x = +1$ have the same stability. However, if $\alpha \neq 0$ (i.e., $-1 < \alpha < 0$ or $0 < \alpha < 1$), it is an asymmetric bistable system. The two steady states $x = -1$ and $x = +1$ have the different stability. For example, if $-1 < \alpha < 0$, the solution $x = +1$ is more stable, oppositely if $0 < \alpha < 1$, the solution $x = -1$ is more stable.

With coupling, the equations of the stationary solution $(x_1^*, x_2^*, \ldots, x_N^*)$ are given by

$$0 = -(x_i^* + 1)(x_i^* - \alpha)(x_i^* - 1) + \varepsilon(x_{i+1}^* + x_{i-1}^* - 2x_i^*). \tag{2}$$

With respect to this stationary solution, the linearization equation is

$$\frac{\mathrm{d}y_i}{\mathrm{d}t} = (1 - 3x_i^{*2} + 2\alpha x_i^*)y_i + \varepsilon(y_{i+1} + y_{i-1} - 2y_i), \tag{3}$$

which can be further written in a compact form as

$$\frac{\mathrm{d}y}{\mathrm{d}t} = Ay,$$

where $y = (y_1, y_2, \ldots, y_N)'$ and

$$A = \begin{pmatrix} 1 - 3x_1^{*2} + 2\alpha x_1^* - 2\varepsilon & \varepsilon & 0 & \ldots & \varepsilon \\ \varepsilon & 1 - 3x_2^{*2} + 2\alpha x_2^* - 2\varepsilon & \varepsilon & \ldots & 0 \\ \ldots & \ldots & \ldots & \ldots & \ldots \\ \varepsilon & 0 & \ldots & \varepsilon & 1 - 3x_N^{*2} + 2\alpha x_N^* - 2\varepsilon \end{pmatrix}. \tag{4}$$

The stability of the stationary solutions is determined by the eigenvalues of the above linearized matrix A. The A is a real symmetric matrix, and thus all its eigenvalues are real. Denoting all N eigenvalues of A as $\lambda_0, \lambda_1, \ldots, \lambda_{N-1}$, with $\lambda_{\max}$ being the maximum among all λ_i's, we have: if $\lambda_{\max} < 0$, the stationary state is stable, otherwise it is unstable.

Generally speaking, the forms of the stationary solutions and the corresponding eigenvalues of their linearized matrix cannot be obtained easily, except for some special cases. For example, if $x_1^* = x_2^* = \cdots = x_N^* = x^*$ (the so-called homogeneous stationary state), we immediately have $\lambda_{\max} = 1 - 3x^{*2} + 2\alpha x^*$, which shows that the homogeneous stationary state $x^* = -1$ (or $x^* = +1$) is stable and $x^* = \alpha$ is unstable for the whole parameters ($-1 < \alpha < 1$ and $\varepsilon > 0$). Clearly they ($x^* = -1$, $x^* = +1$, and $x^* = \alpha$) have the same stability as the steady states in a single system without coupling. Analytical results for some other special cases are also available, which, however, are of no interest in our study, as we are more concerned with general structure of station-

ary patterns from random initial conditions in large coupled systems.

Based on the above analysis, we also find that if $\alpha = 0$ for the symmetric bistable model, the stationary solution $(x_1^*, x_2^*, \ldots, x_N^*)$ and its corresponding antiphase solution $(-x_1^*, -x_2^*, \ldots, -x_N^*)$ have the same stability, and this relation is immediately broken for $\alpha \neq 0$. This property gives a convenience for the analysis if $\alpha = 0$, as we will see below.

As the first step, the phase diagram on the α–ε plane is illustrated in Fig. 1, which shows that stationary patterns exist in the propagation failure (shaded) parameter region, while traveling waves exist in the outer (unshaded) regions. The system size $N = 1000$ is fixed throughout the paper and the results are unchanged for other large N. The coupled equations (1) were solved by using a fourth order Runge–Kutta method with a fixed time step 0.01. The two critical curves determing the final system's dynamics — either stationary patterns or traveling waves were numerically determined. From the picture, clearly $\varepsilon_c(\alpha)$ is finite for $\alpha \neq 0$ and it goes infinite for $\alpha = 0$. The key effect of the diffusive coupling strength ε is it will make one of the two steady states $x = -1$ and $x = +1$, which are locally stable, be globally stable, respectively, if ε is larger than $\varepsilon_c(\alpha)$ for a certain α ($\alpha \neq 0$). Thus, the phenomenon of traveling waves appears out of the propagation failure parameter region and above the critical curves. If $\alpha > 0$ ($\alpha < 0$), $x = -1$ ($x = +1$) will be the final global state. Note that for other types of bistable systems, the phenomenon of a traveling front can still be found in an array of coupled symmetric oscillators, such as in bistable Lorenz oscillators.[28,29]

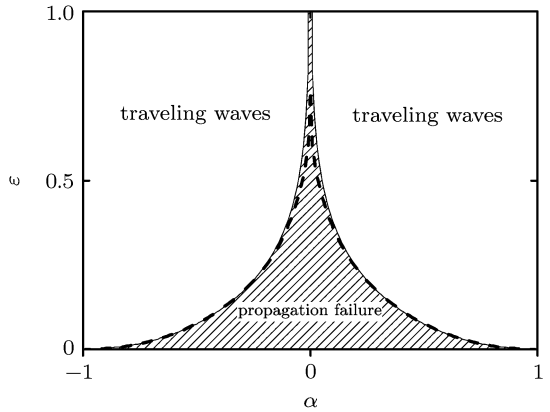


Fig. 1. Phase diagram on the α vs. ε plane for the propagation failure region (the shaded area) and the traveling waves region (the unshaded area). Stationary patterns can be observed within the propagation failure region. A theoretical estimation (dashed lines) for the critical curves is plotted.

In contrast, we give a theoretical estimation (dashed lines)

$$\varepsilon_c = \frac{1}{4}(|\alpha| + 3)(|\alpha| + 1 - 2\sqrt{|\alpha|}), \tag{5}$$

for $-1 < \alpha < 1$, which comes from Ref. [20] analysing the coupled equations (1) from a physical point of view and including dissipative effects. This is expected to be a more precise estimation, compared to the theoretical results of others.[17–19] For more details of derivation and discussion, see Ref. [20].

Within the propagation failure parameter region, rich stationary patterns are expected due to the interaction and competition of the coupled bistable elements. Different from most of the previous works concentrating on propagation waves, the critical (pining–depining) curve, or stationary patterns in the limit of weak coupling by mathematically rigorous analyses,[23, 26] in this work we are more interested in the formation of stationary patterns directly from a phenomenological observation. Our work establishes that very rich stationary patterns are self-organized, which can be well predicted by a simple approximation, the mode analysis method.

3. Stationary patterns in symmetric bistable systems and mode analysis

In this section, we will study the stationary patterns in symmetric bistable systems for $\alpha = 0$. The result can be easily extended to the asymmetric bistable systems for $\alpha \neq 0$, which will be the subject of the next section.

To obtain a global view of stationary patterns with the change of the coupling strength ε ($0 \leq \varepsilon \leq 1.5$), we calculated the bifurcation diagram and the corresponding maximum Lyapunov exponent $\lambda_{\max}$ versus ε. The results are shown in Figs. 2(a) and 2(b), respectively. $N = 1000$ and $\alpha = 0$. In the bifurcation diagram, for each ε the data of the final stationary states for each x_i are plotted. The numerical computational method for $\lambda_{\max}$, based on the coupled equations (1) and the linearization equation (4), is standard.[30] From these pictures, we can see that in the bifurcation diagram (tree) some short branches are born from the main branches and become broken suddenly at certain coupling strengths, where $\lambda_{\max}$ also drops correspondingly. An unusual brushlike bifurcation pattern and a zigzag structure of $\lambda_{\max}$ can

be observed. All these show the organization of the coupled bistable systems and need an explanation.

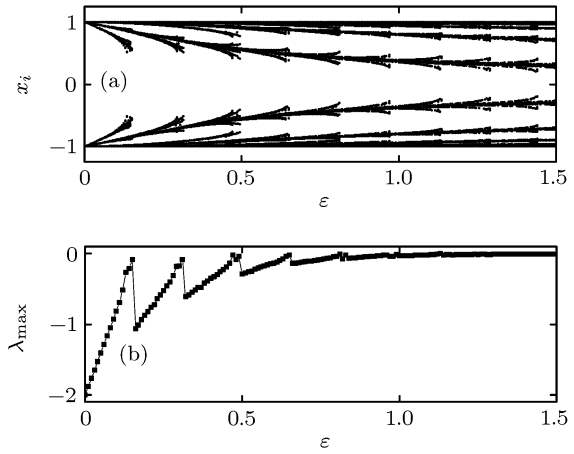


Fig. 2. The bifurcation diagram (a) and the corresponding $\lambda_{\max}$ (b) vs. ε in the coupled bistable equations (1). Random initial conditions are uniformly chosen within $(-1, 1)$. $N = 1000$ and $\alpha = 0$.

For clarity, figure 3 plots the snapshot of the coupled equations at one coupling strength for $\varepsilon = 0.5$ and $N = 1000$. From Figs. 3(a)–3(d), each sub-figure shows only one-fourth part of the whole systems: (a) $i \in [1, 250]$, (b) $i \in [250, 500]$, (c) $i \in [500, 750]$, and (d) $i \in [750, 1000]$. Clearly, lots of elements fall into the two states at $x = -1$ and $x = +1$, forming the upper and lower platforms. Apart from the platforms, two local regular modules (kink and pulse) are seemingly randomly embedded in the platforms. The kink, which acts as a bridge connecting the upper and the lower platforms, is obviously distinct with the pulse, standing on the same platform (either the upper or the lower one). In this respect, we may refer to the localized coherent structure (kink or pulse) in space as an independent mode. As an illustration, a kink and a pulse are emphasized and encircled by the rectangular boxes in Figs. 3(c) and 3(d), respectively. Note that the kink and pulse mode structures in continuous and discrete bistable equations have already been well known. It is our contribution to go further from these qualitative observations, and study their solutions separately and analyse their stabilities in a quantitative way. Although the homogeneous stationary state at $x = -1$ (or $x = +1$) is stable according to our previous analysis, the disordered stationary patterns with the two platforms plus kinks and pulses are commonly observed. For different random initial conditions, we can obtain different patterns, but the global structure and the detailed mode structures remain unchanged. We also find that as the coupling increases, both the kink and pulse structures get wider and occupy more system sites in space.

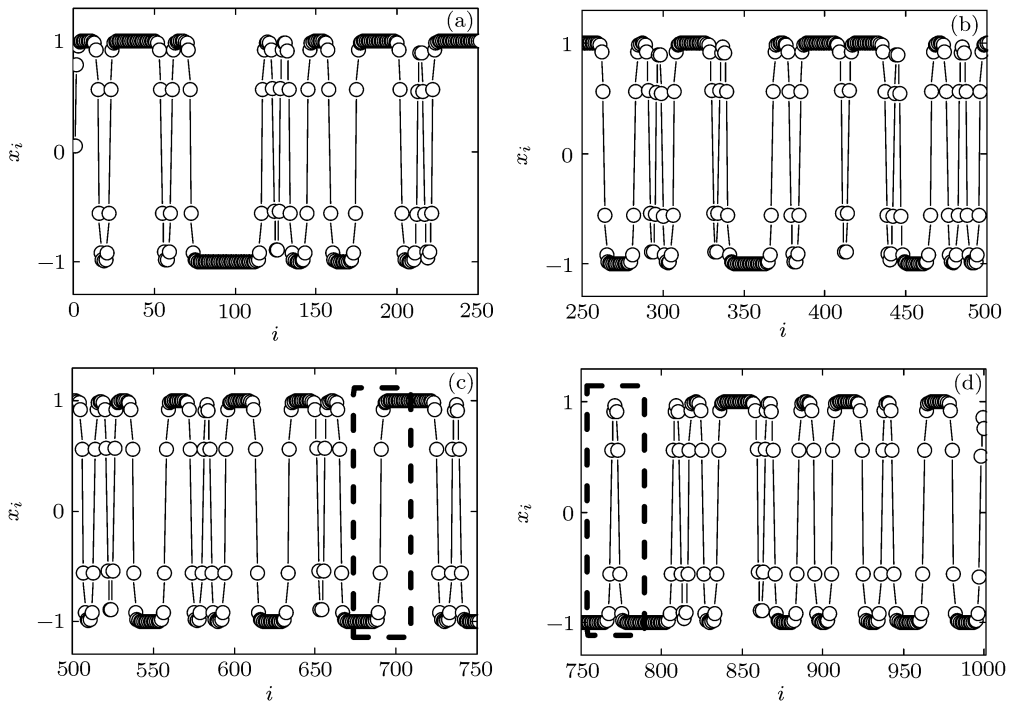


Fig. 3. Stationary patterns of coupled bistable equations (1). The cellular mode structures (kink and pulse) are emphasized in the rectangular boxes in (c) and (d), respectively. $N = 1000$, $\varepsilon = 0.5$, and $\alpha = 0$. From (a) to (d), each sub-figure shows only one-fourth part of the whole system.

As a result, we may cut these mode structures from the whole systems for more detailed studies and obtain the knowledge of large systems from the analysis of these several small systems. This is just the main idea of the mode analysis. The same method has been recently developed in the study of pattern formation in coupled periodic map lattices in our group.[31] To quantitatively characterize the kinks and pulses, we define the mode number $M_{\rm k}$ for kinks as the number of elements moving into the middle region, and the mode number $M_{\rm p}$ for pulses as the number of sites above the unstable state $x = \alpha = 0$. The kink connects the two different platforms at $x = -1$ and $x = +1$; the pulse stands on the same platform, whose position can be either $x = -1$ or $x = +1$. Without losing generality, we choose $x = -1$ (the lower platform). The pulse solution standing on $x = +1$ (the upper platform) can be thought of as the corresponding antiphase solution and can be easily obtained with different signs. Here $\alpha = 0$. For $\alpha \neq 0$, we have to study all pulses (peaks and dips), as we will see in the next section. The schematic shows for the even and odd mode numbers for the kink and pulse are given in Fig. 4. The $M_{\rm k} = 2$ and $M_{\rm k} = 3$ are chosen in Figs. 4(a) and 4(b), respectively, whereas $M_{\rm p} = 2$ and $M_{\rm p} = 3$ in Figs. 4(c) and 4(d), respectively. As odd modes for kink are always unstable and can transfer to the nearest even modes of kink under any small perturbation, they will not be considered further.

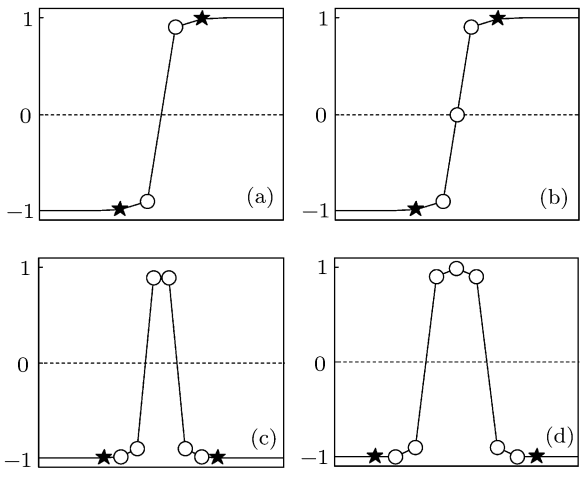


Fig. 4. Schematic illustrations for the kink $M_{\rm k}$ and the pulse $M_{\rm p}$ modes: (a) $M_{\rm k} = 2$; (b) $M_{\rm k} = 3$; (c) $M_{\rm p} = 2$; (d) $M_{\rm p} = 3$. The unknown sites are denoted by open circles, while the fixed boundaries are denoted by stars. The abscissa represents the spatial position of lattice i, and the ordinate represents the corresponding variable x_i. For more details about the definition of the kink and pulse modes for specific mode number, see the text.

Further the coupled equations for small systems governed by the modes of kink (or pulse) can be written as

$$\begin{aligned}\frac{{\rm d}x_i}{{\rm d}t} &= -(x_i+1)(x_i-\alpha)(x_i-1)\\ &\quad + \varepsilon(x_{i+1}+x_{i-1}-2x_i),\\ &\quad i = 2,\ldots,L-1 \end{aligned} \tag{6}$$

with different fixed boundary conditions: for the kink mode $M_{\rm k}$, $x_1 = -1$ and $x_L = +1$, and $L = M_{\rm k} + 2$; for the pulse mode $M_{\rm p}$, $x_1 = -1$ and $x_L = -1$, and L should be sufficiently large ($L \gg M_{\rm p} + 2$).

The simulation results for the kink and pulse are displayed in Figs. 5 and 6, respectively. In numerics, special initial conditions have been chosen to obtain the proper mode structures and eliminate the effect of multiple stationary states for different initial conditions. For the (even-number) kink, each x_i for $i = 2,\ldots,L/2$ is set to an arbitrary negative number, and each x_i for $L/2+1,\ldots,L-1$ is set to an arbitrary positive number, $-1 \leq x_i \leq 1$ for all lattices. For the pulse, the middle $M_{\rm p}$ lattices have been set to be positive randomly, with others negative, $L = 20$ is usually chosen. This manipulation guarantees that the final state can fall into the mode structure after a transient is discarded. For the schematic illustration, see Fig. 4. In Figs. 5(a)–5(f), we plot the bifurcation diagrams for $M_{\rm k} = 2, 4, 6, 8, 10$, and 12, respectively. We can see that the number of the branches increases for larger $M_{\rm k}$ mode, which means that with increase of the coupling, more elements move into the middle regions and the kink gets wider. We also find that if $M_{\rm k}$'s are sufficiently large, there is no much difference between them, e.g., the bifurcation diagrams for the modes $M_{\rm k} = 8, 10$, and 12 are nearly the same in the parameter region $0 \leq \varepsilon \leq 1.5$ [compare the curves in Figs. 5(d)–5(f)]. Therefore, we only need to consider the $M_{\rm k} = 10$ mode in the following.

Similarly, we plot the bifurcation diagrams for the pulse modes from $M_{\rm p} = 1$ to 10 in Figs. 6(a)–6(j). Clearly, the number of branches also increases for large $M_{\rm p}$. Nevertheless, different from the splitting behaviour of the kink modes in Fig. 5, the bifurcation branches of the pulse modes vanish abruptly once the coupling exceeds a certain critical value. With the increase of coupling, this disappearance occurs gradually for all pulses from small $M_{\rm p}$ to large ones.

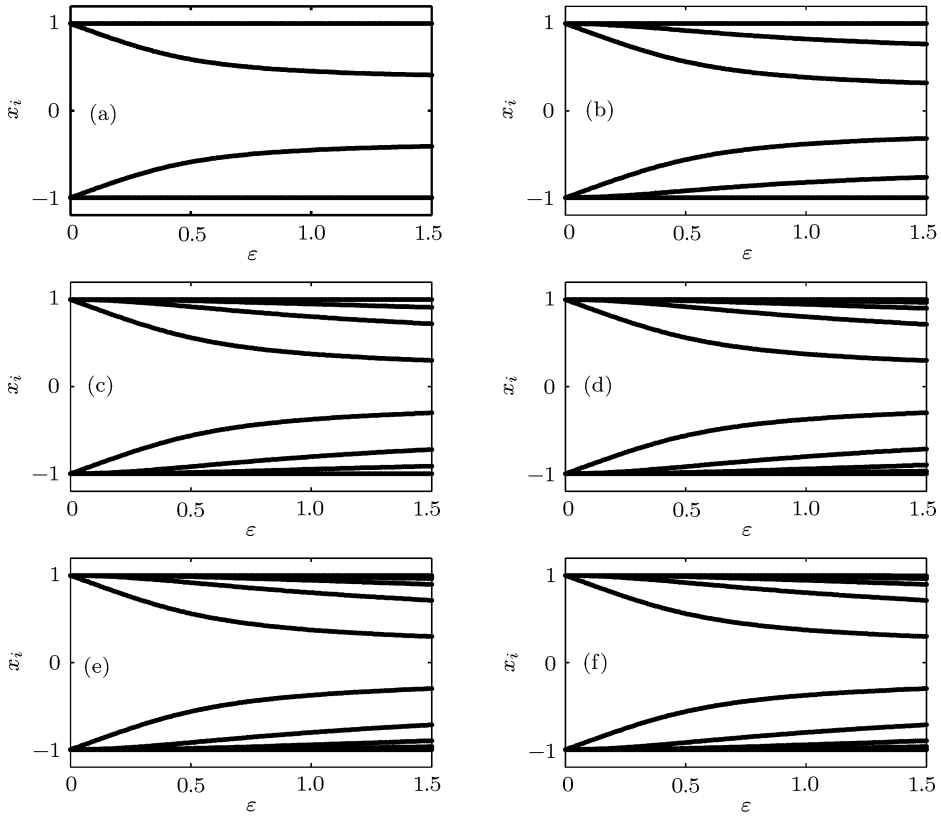
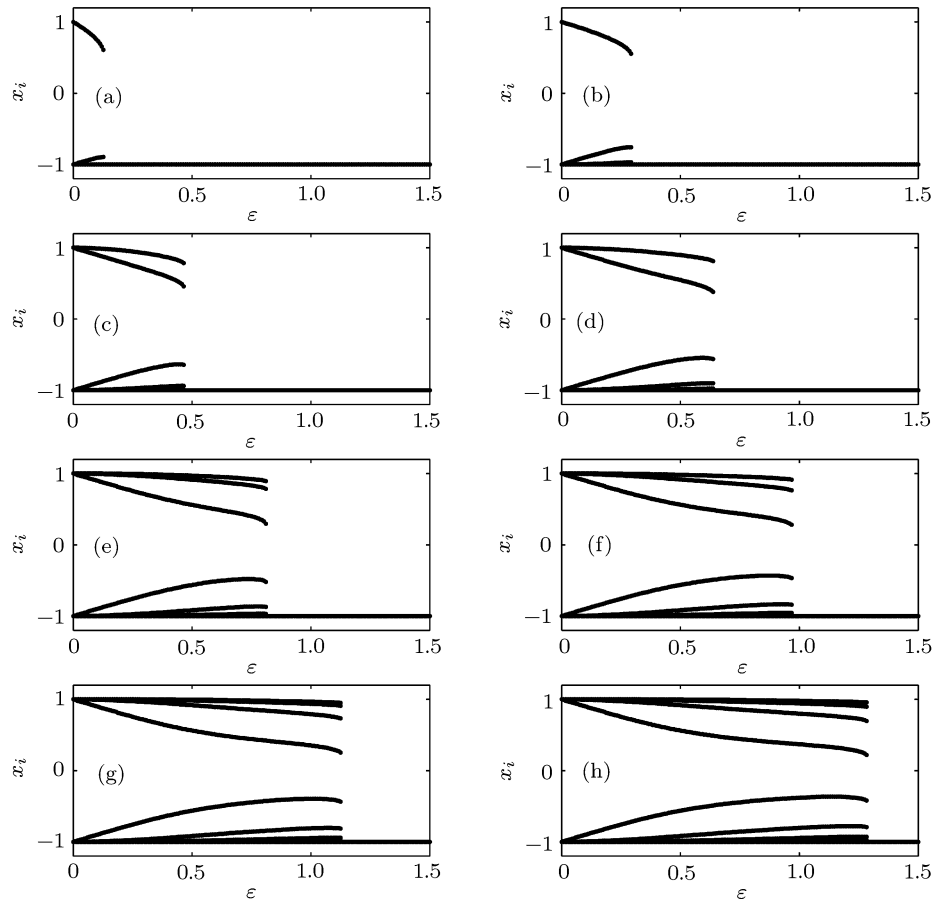


Fig. 5. The bifurcation diagrams of the kink for the different mode numbers $M_{\rm k} = 2$, 4, 6, 8, 10, and 12, respectively, (a)–(f). They are obtained from the integration of the mode equation (6) for each mode number $M_{\rm k}$.



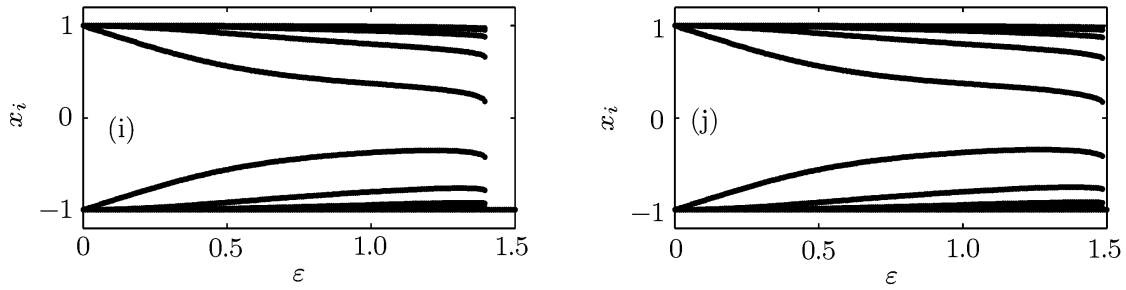


Fig. 6. The same as Fig. 5 for the pulse number $M_{\rm p}$ from 1 to 10 instead (subfigures (a)–(j)).

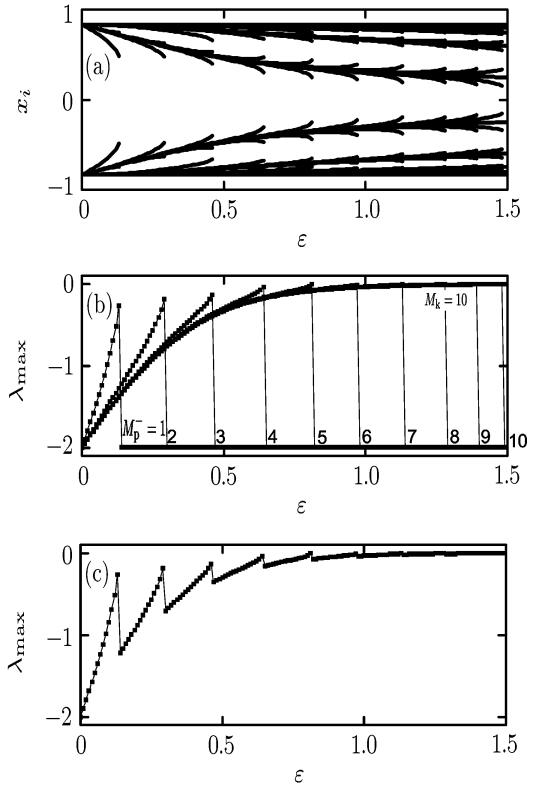


Fig. 7. (a) The bifurcation diagrams for the kink and pulse including $M_{\rm k} = 10$ and $M_{\rm p}$ (from 1 to 10) and their corresponding antiphase solutions. Subfigures (b) and (c) show the corresponding $\lambda_{\max}$'s of these modes and their maximum value vs. ε, respectively. In (b), $\lambda_{\max}$ for each $M_{\rm k}$ or $M_{\rm p}$ was calculated based on the corresponding (mode) coupled equation (6) and its linearization equation. This is different from the calculation of $\lambda_{\max}$ in Fig. 2(b).

We plot all the bifurcation diagrams of $M_{\rm k} = 10$ [Fig. 5(e)] and $M_{\rm p}$ from 1 to 10 (Fig. 6) in Fig. 7(a). All of the antiphase solutions of pulses are added. Apparently, the pattern is similar to the original bifurcation diagram for the whole coupled large systems [Fig. 2(a)]. It shows that the kink mode contributes to the trunks and the pulses contribute to the broken branches. We also calculated the $\lambda_{\max}$ for each mode. The results are given in Fig. 7(b). The largest value among all the modes is chosen and plotted in Fig. 7(c); the pattern is quite similar to the $\lambda_{\max}$ of the coupled systems in Fig. 2(b). Since the mode analysis method is only an approximation theory, it is discernible that the predicted values for the thresholds of $\lambda_{\max}$ appear a little earlier than the real values.

Our further researches revealed that the pulses lose stability through a tangent bifurcation. The results are shown in Fig. 8, as $M_{\rm p} = 1$ and 2 for example, with the bifurcation diagrams in Figs. 8(a) and 8(b), and their corresponding $\lambda_{\max}$ in Figs. 8(c) and 8(d). The stable (unstable) solutions are denoted by thick (thin) line. Clearly, the stable branches of the pulse collide with the branches of the unstable solution at a certain critical parameter, and both are annihilated immediately, this is indicative of the properties of tangent bifurcation. Different from the Runge–Kutta method directly integrating the pulse differential equations (6), here the Newton–Raphson algorithm[28] is performed, with which both stable and unstable solutions can be obtained.

All the results suggest that the kink and pulse play constructive but distinct roles in the stationary patterns of the coupled systems, and compared with the modest effect of kink with more branches splitting out with increase of the coupling, the effect of pulse is more severe with the mode structure becoming unstable and vanishing through tangent bifurcation.

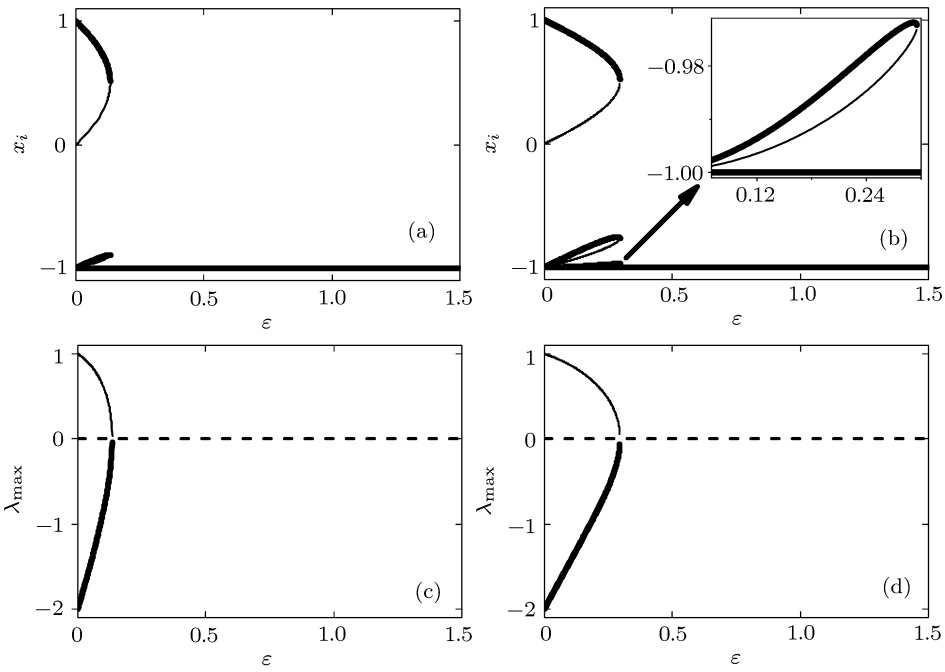


Fig. 8. The mechanism for the instability of the pulse modes. Subfigures (a) and (b) are the same as Figs. 6(a) and 6(b) for the pulse numbers $M_{\rm p} = 1$ and $M_{\rm p} = 2$, respectively, but with both the stable (thick) and unstable (thin) solutions included. The insert in (b) is the enlargement of the left lower part. Subfigures (c) and (d) are the corresponding $\lambda_{\max}$ versus ε. The stable and unstable solution branches collide and disappear at the critical coupling, reflecting the tangent bifurcation nature.

4. Stationary patterns in asymmetric bistable systems and mode analysis

In this section, we turn our attention to the coupled asymmetric bistable systems for $\alpha \neq 0$. We will see that the mode analysis still works. Under this situation, the symmetric structure of the pulse and its antiphase solution does not exist, and thus we have to consider all pulse modes standing on the lower platform at $x = -1$ (peaks) and those standing on the upper platform at $x = +1$ (dips) separately. We may classify these two structures by using $M_{\rm p}^-$ and $M_{\rm p}^+$, respectively. For kinks, however, this manipulation is unnecessary.

The bifurcation diagram of the coupled equations (1) and the theoretical result from the mode analysis (6) considering the first several important low modes ($M_{\rm k} = 10, M_{\rm p}^- = 1, 2, 3$, and $M_{\rm p}^+ = 1$) are shown in Figs. 9(a) and 9(b), respectively. Clearly, they are in good agreement. Here $\alpha = 0.1$; for other nonzero α's, we obtain similar results. As $\alpha \neq 0$, a critical coupling strength ($\varepsilon_{\rm c} \simeq 0.38$) exists, after which the whole systems move into the traveling wave parameter region (Fig. 1) and fall into the homogeneous stationary state at $x = -1$ after a transient time. Naturally, we also obtain a good prediction for the $\lambda_{\max}$ pattern, as shown in Fig. 10.

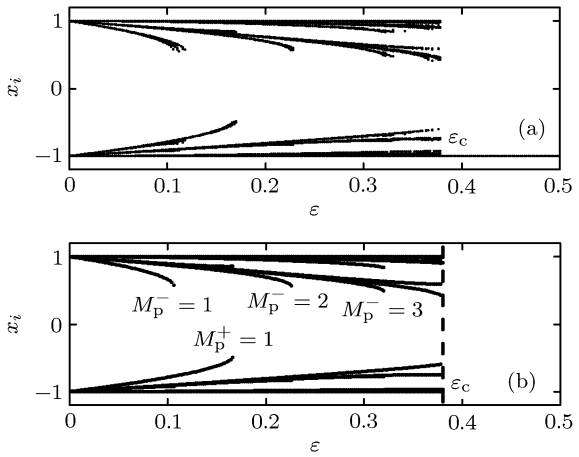


Fig. 9. The study of mode analysis on asymmetric bistable systems [Eq. (1) for $\alpha \neq 0$], showing the validation and efficiency of the method for any α. Subfigures (a) and (b) are the bifurcation diagrams of the coupled equations (1) and the mode equations (6) for $M_{\rm k} = 10, M_{\rm p}^- = 1, 2, 3$, and $M_{\rm p}^+ = 1$, respectively, $\alpha = 0.1$.

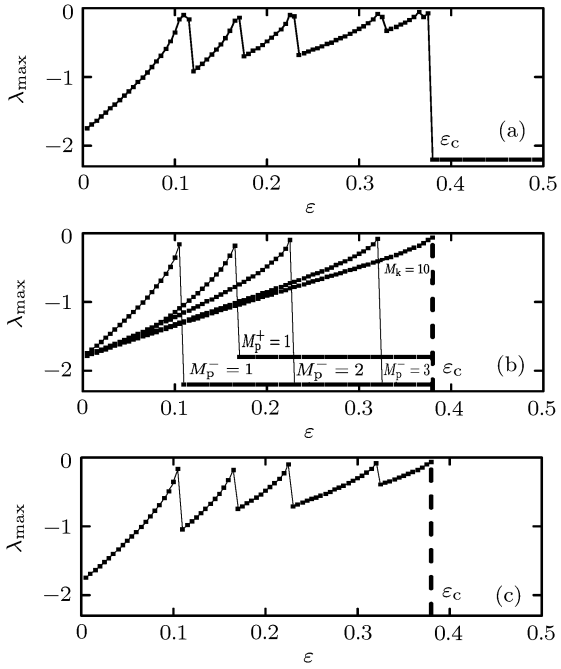


Fig. 10. Subfigures (a), (b), and (c) show $\lambda_{\max}$ of the coupled equations (1), $\lambda_{\max}$'s of the mode equations (6) for $M_k = 10, M_p^- = 1, 2, 3$, and $M_p^+ = 1$, and their maximum value vs. ε, respectively, $\alpha = 0.1$. For $\varepsilon > \varepsilon_c \approx 0.38$, the pattern becomes non-stationary and a traveling wave behaviour appears.

5. Conclusion and discussion

In this work, we have systematically studied the stationary patterns in a discrete bistable system. A mode analysis method allows us to cut the whole large systems into several independent modes (kink and pulse) for detailed analysis. The different roles of kink and pulse have been well recognized. Therefore, the structure, formation, and stability of these stationary patterns have been well characterized. Below it is necessary to give some discussions.

(i) The findings are very generic. Similar results have been found in multi-variable bistable systems, such as the Fitz–Hugh–Naguma model and Lorenz model, and other multistable systems with the coexistence of more than two stable steady states. In all these cases, the mode analysis has been proved successful.

(ii) In the discrete bistable media, within the traveling wave parameter region, one expects to find traveling kinks (fronts) but not usually traveling pulses.[6] In contrast, within the propagation failure parameter region, both stationary kinks and stationary pulses are observed.

(iii) Our mode analysis is an approximate method, based on simple observation of mode structures of stationary patterns in discrete bistable systems. It is fundamentally different with the analysis of homo- and heteroclinic connections, which is standard for calculation of localized patterns (pulses and kinks, respectively) in continuous bistable systems.[6] For continuous bistable systems, the effects of parameters in the reaction and diffusive terms have been analysed in detail mathematically and physically.[6] It is, however, difficult to generalize the method and obtain similar rigorous results in discrete bistable systems. For more discussions, see Ref. [6].

(iv) In numerics, the system size $N = 1000$ is used. The pattern configuration may change with different N, but the mode structures are unchanged for any large N. However, for small N, e.g., $N = 8$ or $N = 10$, the mode structures may not be observed.

(v) Finally, it is interesting to briefly compare stationary Turing pattern in monostable media and stationary pattern in bistable media. The former pattern occurs from a homogeneous stationary state by a diffusion-induced bifurcation and shows a periodicity in space. A finite coupling strength is needed for the appearance. In contrast, the stationary pattern in bistable media occurs due to the competition of the two stable steady states and show a global randomness in space and a local regularity with well-organized kink and pulse structures. Correspondingly, it is only observable for the coupling smaller than a certain threshold.

We hope all these findings and results are of significance and importance for our understanding of patterns in nature.

References

[1] Cross M C and Hohenberg P C 1993 *Rev. Mod. Phys.* **65** 851

[2] Kapral R and Showalter K 1995 *Chemical Waves and Patterns* (Dordrecht: Kluver Academic Publishers)

[3] Epstein I R and Pojman J A 1998 *An Introduction to Nonlinear Chemical Dynamics: Oscillations, Waves, Pat-*

terns, and Chaos (New York: Oxford University Press)
[4] Kuramoto Y 1984 *Chemical Oscillations, Waves, and Turbulence* (Berlin: Springer)
[5] Field R J and Burger M 1985 *Oscillations and Travelling Waves in Chemical Systems* (New York: Wiley-Interscience)
[6] Keener J and Sneyd J 1998 *Mathematical Physiology* (New York: Springer-Verlag) Chapter 9
[7] Murray J D 2003 *Mathematical Biology* 3rd edn. (Berlin: Springer)
[8] Gao Z Y and Lu Q S 2007 *Chin. Phys.* **16** 2479
[9] Wang B Y, Xing Z C and Xu W 2009 *Acta Phys. Sin.* **58** 6590 (in Chinese)
[10] Turing A M 1952 *Philos. Trans. Roy. Soc. London* Ser. B **237** 37
[11] Castets V, Dulos E, Boissonade J and De Kepper P 1990 *Phys. Rev. Lett.* **64** 2953
[12] De Kepper P, Castets V, Dulos E and Boissonade J 1991 *Physica* D **49** 161
[13] Langyel I and Epstein I R 1990 *Science* **251** 650
[14] Ouyang Q and Swinney H L 1991 *Nature* **352** 610
[15] Kladko K, Mitkov I and Bishop A R 2000 *Phys. Rev. Lett.* **84** 4505
[16] Laplante J P and Erneux T 1992 *J. Phys. Chem.* **96** 4931
[17] Erneux T and Nicolis G 1993 *Physica* D **67** 237
[18] Fáth G 1998 *Physica* D **116** 176
[19] Keener J P 1987 *SIAM J. Appl. Math.* **47** 556
[20] Comte J C, Morfu S and Marquié P 2000 *Phys. Rev.* E **64** 027102
[21] Mitkov I, Kladko K and Pearson J E 1998 *Phys. Rev. Lett.* **81** 5453
[22] Preez-Munuzuri V, Perez-Villar V and Chua L O 1992 *Int. J. Bifur. Chaos* **2** 403
[23] MacKay R S and Sepulchre J A 1995 *Physica* D **82** 243
[24] Nekorkin V I and Makarov V A 1995 *Phys. Rev. Lett.* **74** 4819
[25] Muñuzhi A P and Chua L O 1997 *Int. J. Bifur. Chaos* **7** 2807
[26] Nizhnik L P, Nizhnik I L and Hasler M 2002 *Int. J. Bifur. Chaos* **12** 261
[27] Nagumo J, Arimoto S and Yoshisawa S 1962 *Proc. IRE* **50** 2061
[28] Pazó D and Pérez-Muñuzuri V 2001 *Phys. Rev.* E **64** 065203(R)
[29] Pazó D and Pérez-Muñuzuri V 2003 *Chaos* **13** 812
[30] Parker T S and Chua L O 1989 *Practical Numerical Algorithms for Chaotic Systems* (New York: Springer-Verlag)
[31] Liu W Q, Wu Y, Zou W, Xiao J H and Zhan M 2007 *Phys. Rev.* E **76** 036215